Figure S1

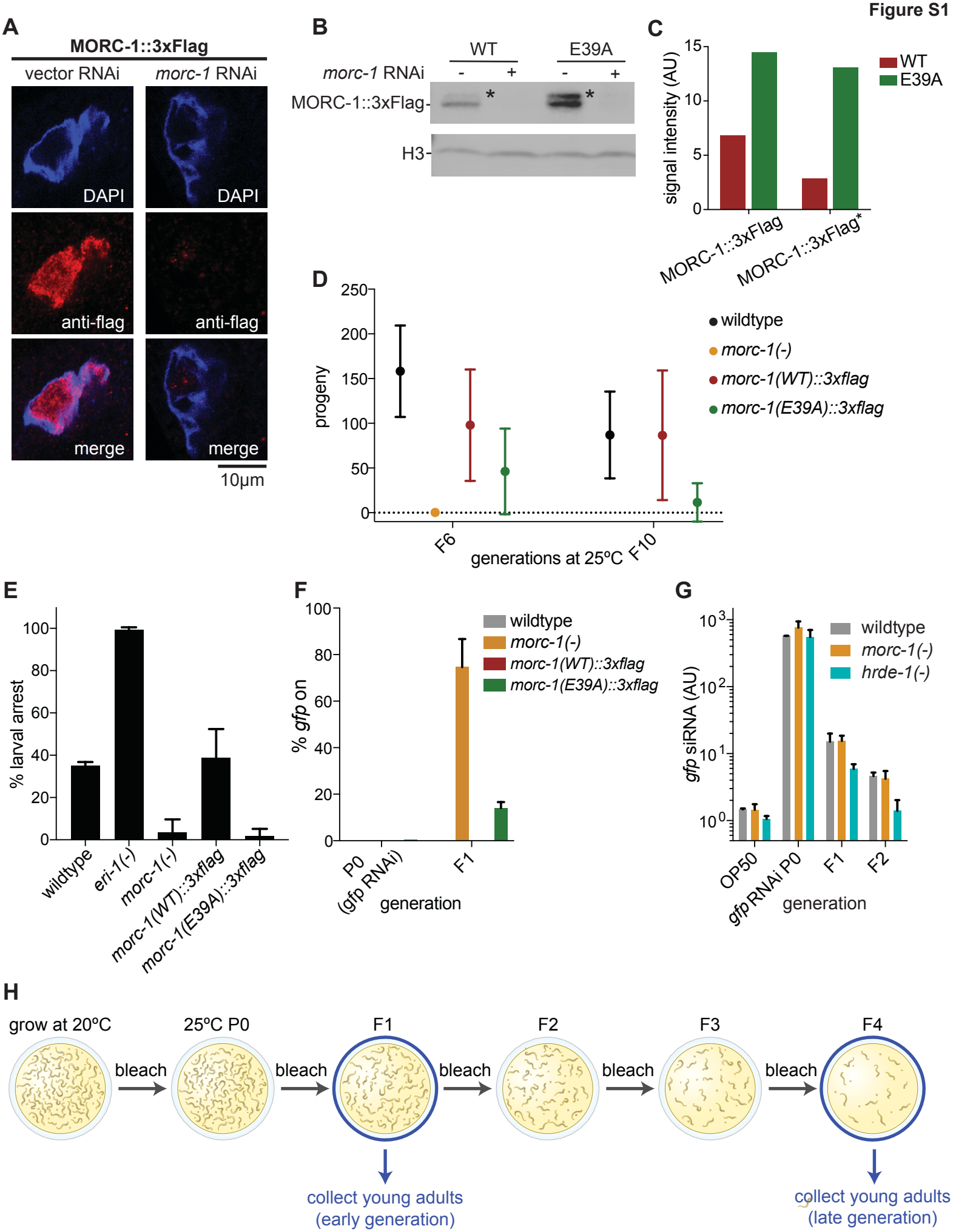
A
MORC-1::3xFlag
vector RNAi
morc-1 RNAi
DAPI
DAPI
anti-flag
anti-flag
merge
merge
10µm
B
WT
E39A
morc-1 RNAi
- + - +
MORC-1::3xFlag
H3
C
signal intensity (AU)
15
10
5
0
WT
E39A
MORC-1::3xFlag
MORC-1::3xFlag*
D
progeny
250
200
150
100
50
0
wildtype
morc-1(-)
morc-1(WT)::3xflag
morc-1(E39A)::3xflag
F6
F10
generations at 25ºC
E
% larval arrest
100
80
60
40
20
0
wildtype
eri-1(-)
morc-1(-)
morc-1(WT)::3xflag
morc-1(E39A)::3xflag
F
% gfp on
100
80
60
40
20
0
wildtype
morc-1(-)
morc-1(WT)::3xflag
morc-1(E39A)::3xflag
P0 (gfp RNAi)
F1
generation
G
gfp siRNA (AU)
10^3
10^2
10^1
10^0
wildtype
morc-1(-)
hrde-1(-)
OP50
gfp RNAi P0
F1
F2
generation
H
grow at 20ºC
25ºC P0
F1
F2
F3
F4
bleach
bleach
bleach
bleach
bleach
collect young adults (early generation)
collect young adults (late generation)

Figure S1. Related to Figures 1, 2, 3, 5, and 6. MORC-1 is expressed in somatic nuclei, characterization of E39A variant, *morc-1* does not regulate siRNA accumulation, RNA-seq and ChIP-seq strategy overview. (A) MORC-1::3xFlag is expressed in intestinal nuclei shown by anti-Flag immunofluorescence and DAPI staining of worms expressing *morc-1::3xflag* at the endogenous *morc-1* locus and grown for two generations on empty vector RNAi or on *morc-1* RNAi. **(B)** Western blot of worms expressing *morc-1(WT)::3xflag* and *morc-1(E39A)::3xflag* grown on vector or *morc*-1 RNAi using anti-Flag antibody. Anti-H3 antibody was used as a loading control. Asterisk designates a higher molecular weight band that is eliminated by *morc-1* RNAi. This may indicate a post-translational modification or alternative isoform of MORC-1. Quantification of both bands by LI-COR Odyssey Fc is shown in **(C)**. **(D)** Fertility of designated genotype at F6 and F10 generations at 25°C. Mean fertility ± SD of 12 worms per genotype per generation is shown. *morc-1(-)* mutants are sterile at F6, *morc-1(E39A)::3xflag* mutants are essentially sterile at F10, and *morc-1(WT)::3xflag* worms have wildtype fertility. **(E)** *morc-1(E39A)::3xflag* mutants are resistant to *lir-1* RNAi. *morc-1(WT)::3xflag* worms have wildtype sensitivity to *lir-1* RNAi. Bars indicate percentage of worms arrested or dead as a mean of three biological replicates ± SD; n≥100 **(F)** *morc-1(E39A)::3xflag* is defective for RNAi inheritance. On *gfp* RNAi, silencing of *gfp* is completely penetrant, but there is a mild defect in *gfp* silencing in the F1 generation. In *morc-1(-)* mutants, the majority of F1 worms express GFP. Silencing is completely penetrant in P0 and F1 generations in *morc-1(WT)::3xflag* and wildtype worms. Bars indicate percentage of worms expressing GFP as mean of three biological replicates ± SD; n≥50. **(G)** Levels of anti-*gfp* siRNAs in adult worms grown on *gfp* RNAi and in F1 and F2 generations grown on OP50. siRNA levels measured by TaqMan qRT-PCR, normalized to U18, and shown in arbitrary units as mean of two technical replicates ± SD. **(H)** Sample collection schematic for RNA-seq and ChIP-seq studies.

Figure S2

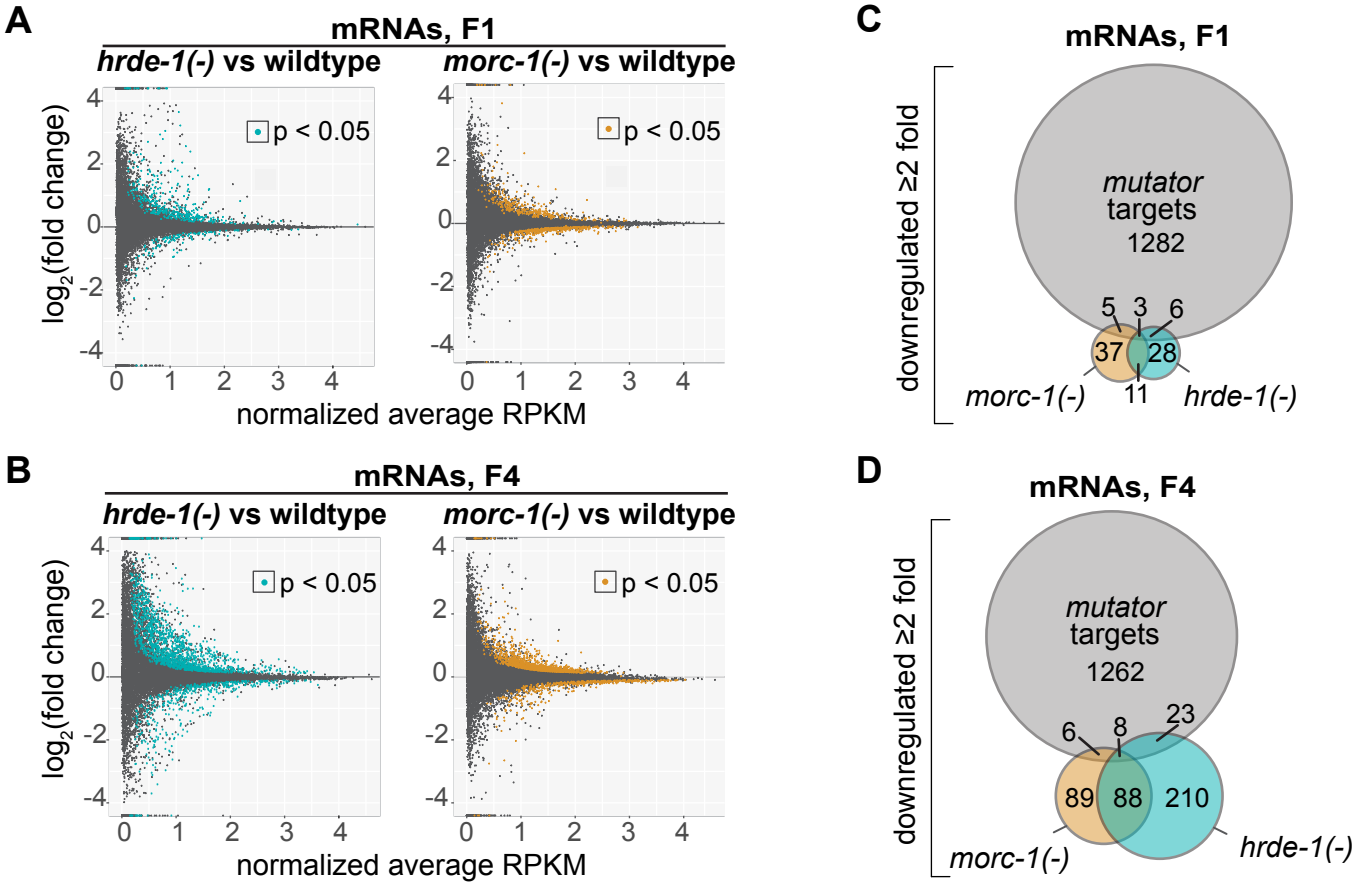
A
mRNAs, F1
hrde-1(-) vs wildtype
morc-1(-) vs wildtype
p < 0.05
log2(fold change)
normalized average RPKM
B
mRNAs, F4
hrde-1(-) vs wildtype
morc-1(-) vs wildtype
p < 0.05
log2(fold change)
normalized average RPKM
C
mRNAs, F1
downregulated ≥2 fold
mutator targets 1282
5
3
6
37
28
11
morc-1(-)
hrde-1(-)
D
mRNAs, F4
downregulated ≥2 fold
mutator targets 1262
6
8
23
89
88
210
morc-1(-)
hrde-1(-)

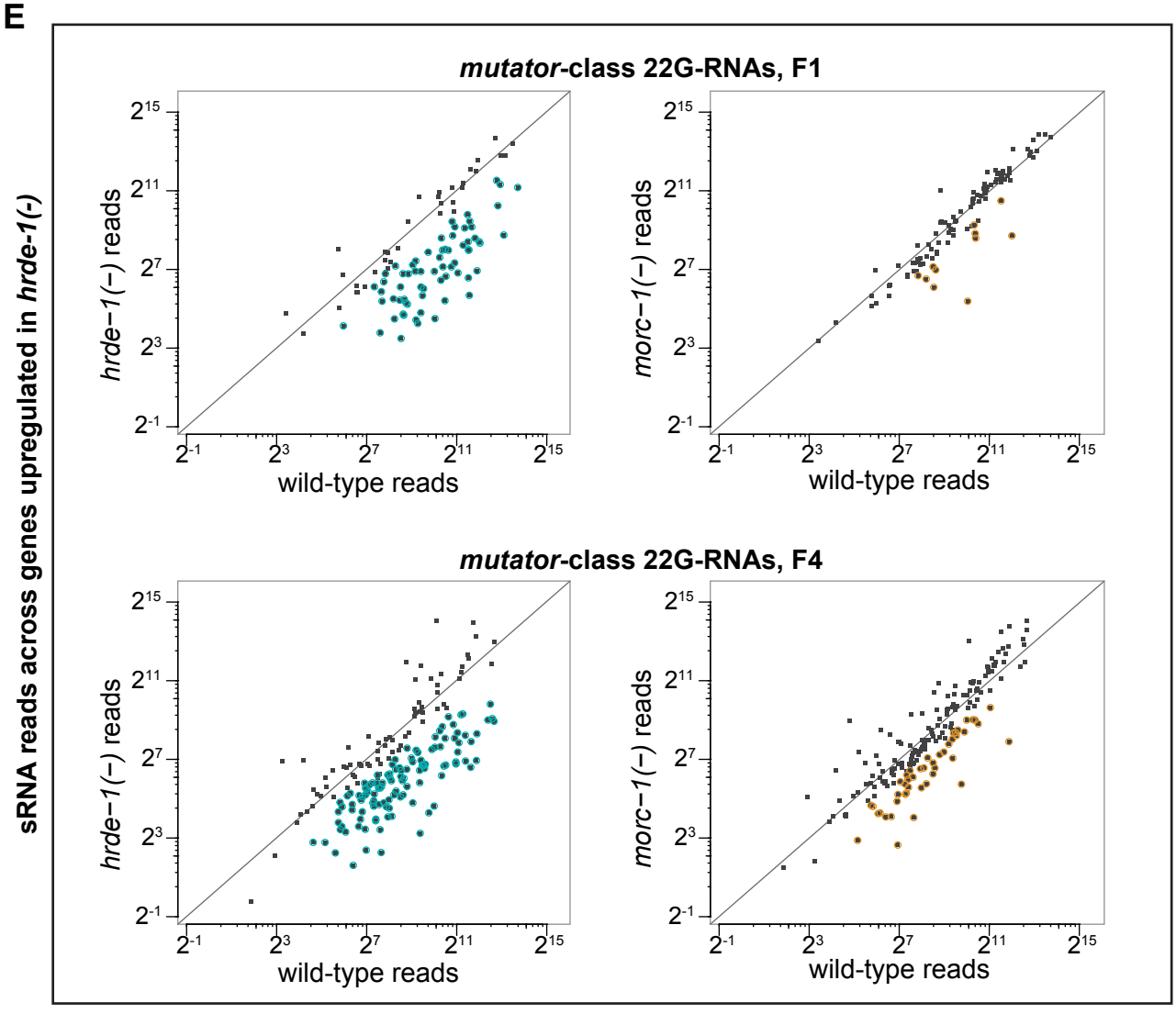
E
sRNA reads across genes upregulated in hrde-1(-)
mutator-class 22G-RNAs, F1
hrde−1(−) reads
morc−1(−) reads
wild-type reads
mutator-class 22G-RNAs, F4
hrde−1(−) reads
morc−1(−) reads
wild-type reads

Figure S2. Related to Figure 2. *morc-1* regulates 22G endo-siRNA targets. (A) Log2(fold change) as a function of normalized average RPKM *hrde-1(-)* (left) and *morc-1(-)* (right) vs. wildtype in F1 generation. mRNAs that are up or down-regulated with p<0.05 in *hrde-1(-)* or *morc-1(-)* are indicated in blue and yellow, respectively. **(B)** Log2(fold change) as a function of normalized average RPKM *hrde-1(-)* (left) and *morc-1(-)* (right) vs. wildtype in F4 generation. mRNAs that are up or down-regulated with p<0.05 in *hrde-1(-)* or *morc-1(-)* are indicated in blue and yellow, respectively. **(C)** Overlap of testable *mutator* targets with downregulated mRNAs in *morc-1(-)* and *hrde-1(-)* in F1 and **(D)** F4. **(E)** 22G endo-siRNA levels corresponding to *mutator* targets that are upregulated in *hrde-1(-)* at F1 (top) and F4 (bottom) in *hrde-1(-)* and *morc-1(-)* vs. wildtype. Significantly depleted 22G endo-siRNAs in *hrde-1(-)* are highlighted in blue; significantly depleted 22G endo-siRNAs in *morc-1(-)* are highlighted in yellow.

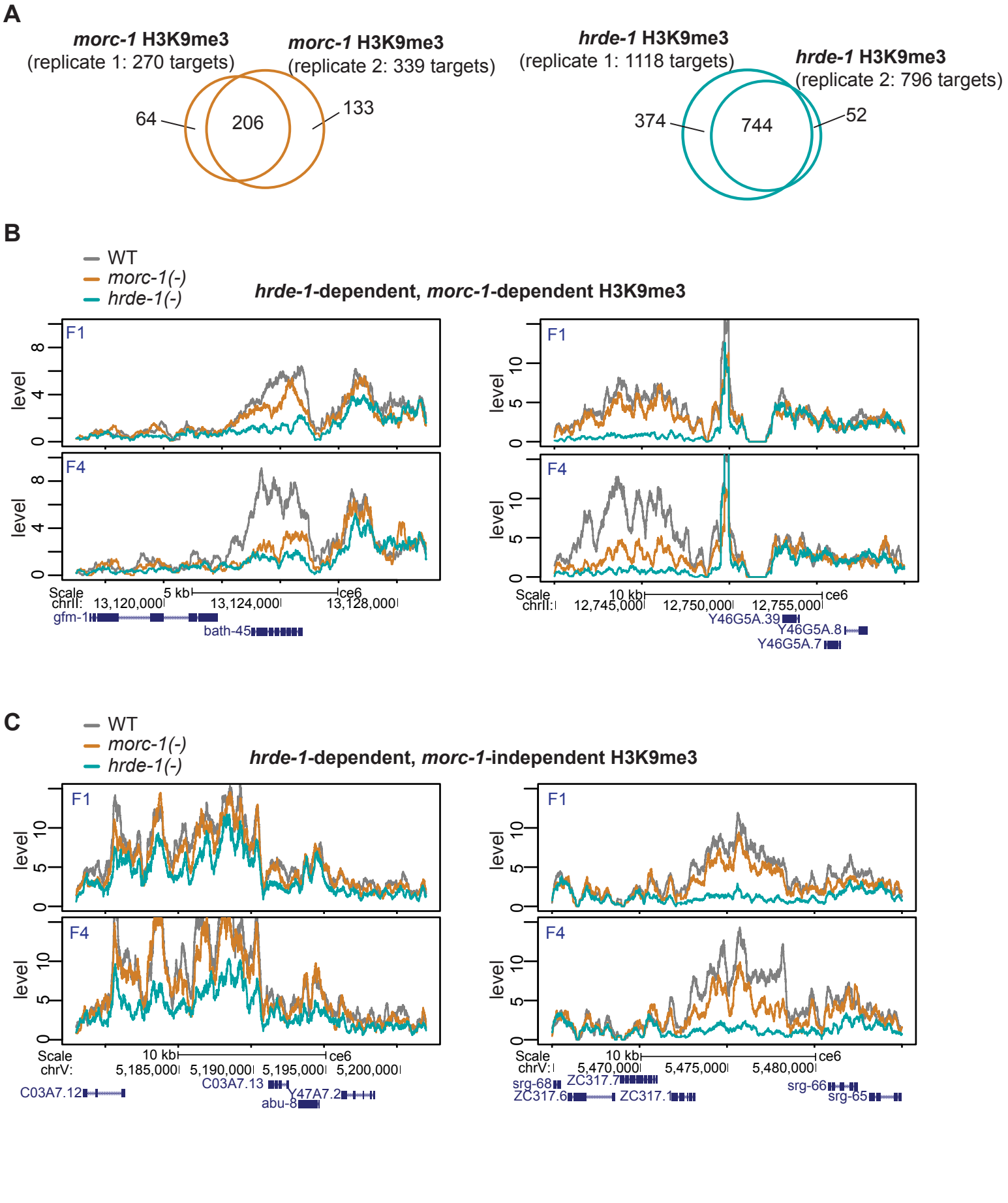
A
morc-1 H3K9me3
(replicate 1: 270 targets)
morc-1 H3K9me3
(replicate 2: 339 targets)
64
206
133
hrde-1 H3K9me3
(replicate 1: 1118 targets)
hrde-1 H3K9me3
(replicate 2: 796 targets)
374
744
52
B
WT
morc-1(-)
hrde-1(-)
hrde-1-dependent, morc-1-dependent H3K9me3
F1
F4
level
Scale
chrII:
13,120,000
5 kb
13,124,000
13,128,000
ce6
gfm-1
bath-45
chrII:
12,745,000
10 kb
12,750,000
12,755,000
Y46G5A.39
Y46G5A.8
Y46G5A.7
C
WT
morc-1(-)
hrde-1(-)
hrde-1-dependent, morc-1-independent H3K9me3
chrV:
5,185,000
10 kb
5,190,000
5,195,000
5,200,000
C03A7.12
C03A7.13
Y47A7.2
abu-8
5,470,000
5,475,000
5,480,000
srg-68
ZC317.7
ZC317.6
ZC317.1
srg-66
srg-65

Figure S3. Related to Figure 3. H3K9me3 replicate overlap and more exemplary regions. (A) Overlap between biological replicates of H3K9me3-depleted regions (fold change >1.5, FDR<0.05) in F4 mutant vs. wildtype (top: *morc-1(-)* vs. wildtype, bottom: *hrde-1(-)* vs. wildtype). Subsequent analyses were performing using sites that were identified in both biological replicates. **(B)** H3K9me3 levels at exemplary *morc-1*-dependent H3K9me3 regions at early and late generation. **(C)** H3K9me3 levels at exemplary *hrde-1*-dependent, *morc-1*-independent H3K9me3 loci at early and late generation.

Figure S4

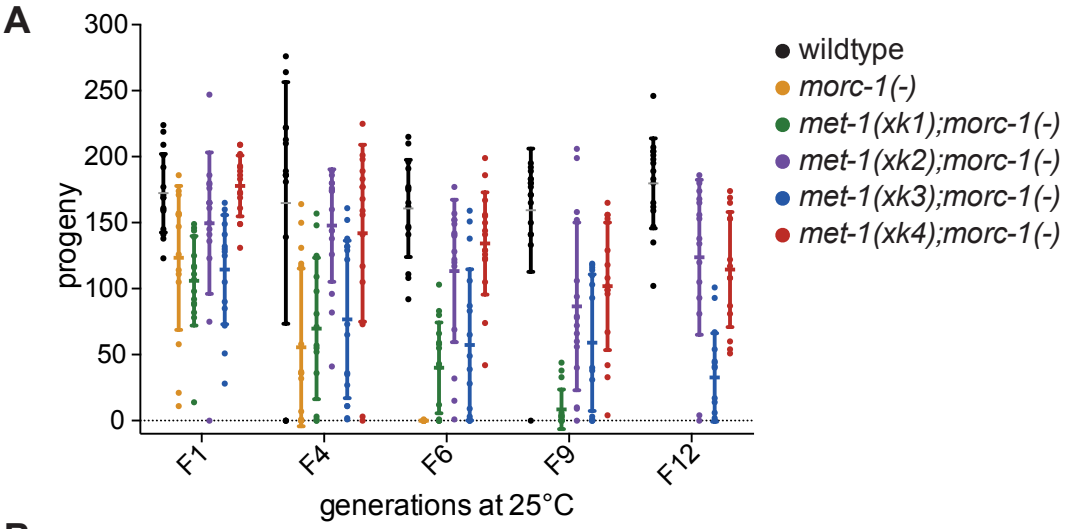
A
300
250
200
150
100
50
0
progeny
F1
F4
F6
F9
F12
generations at 25°C
wildtype
morc-1(-)
met-1(xk1);morc-1(-)
met-1(xk2);morc-1(-)
met-1(xk3);morc-1(-)
met-1(xk4);morc-1(-)

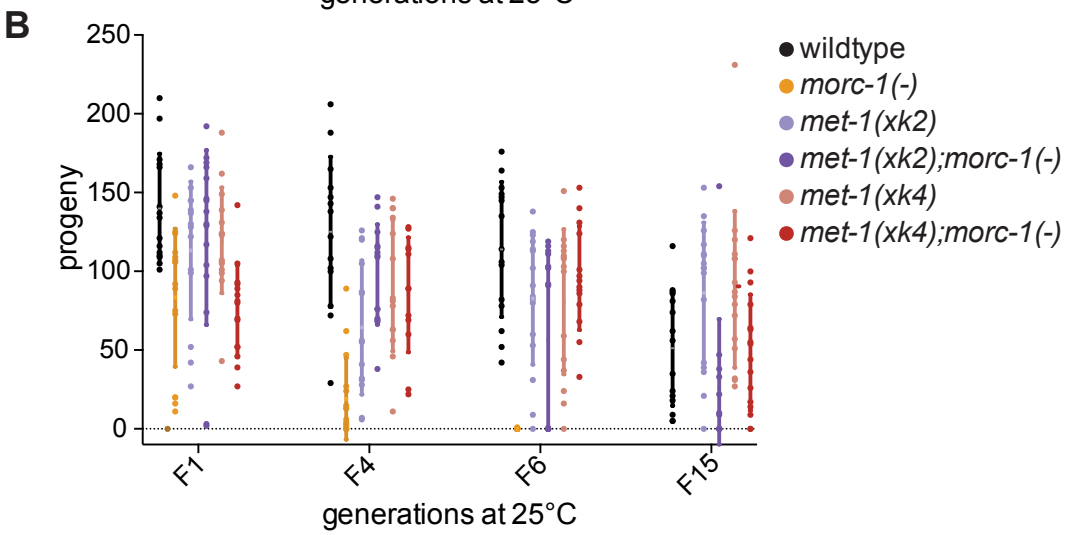
B
250
200
150
100
50
0
progeny
F1
F4
F6
F15
generations at 25°C
wildtype
morc-1(-)
met-1(xk2)
met-1(xk2);morc-1(-)
met-1(xk4)
met-1(xk4);morc-1(-)

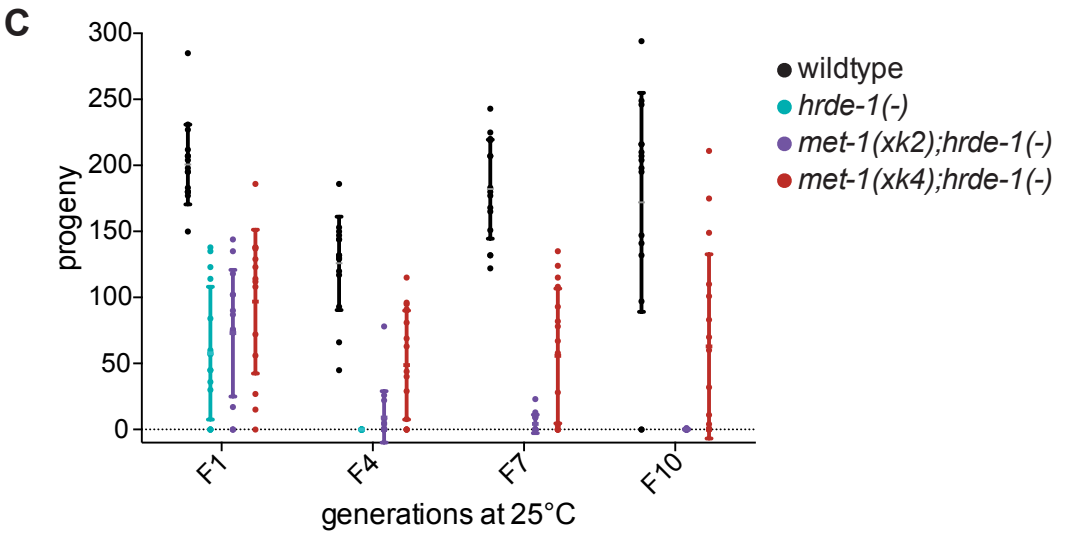
C
300
250
200
150
100
50
0
progeny
F1
F4
F7
F10
generations at 25°C
wildtype
hrde-1(-)
met-1(xk2);hrde-1(-)
met-1(xk4);hrde-1(-)

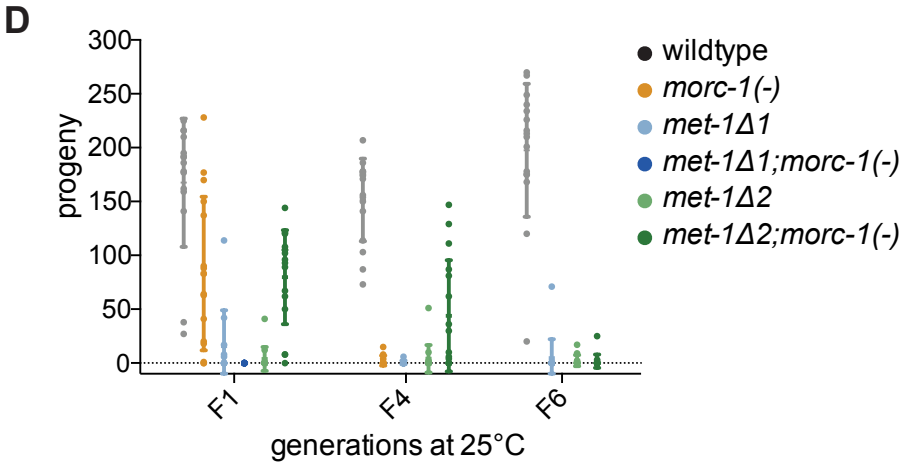
D
300
250
200
150
100
50
0
progeny
F1
F4
F6
generations at 25°C
wildtype
morc-1(-)
met-1Δ1
met-1Δ1;morc-1(-)
met-1Δ2
met-1Δ2;morc-1(-)

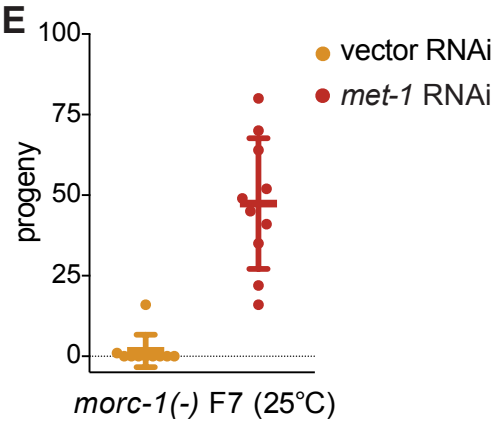
E
100
75
50
25
0
progeny
morc-1(-) F7 (25°C)
vector RNAi
met-1 RNAi

Figure S4. Related to Figure 5. New *met-1* alleles, but not deletion alleles, suppress *morc-1(-)* and *hrde-1(-)* germline mortality. Germline mortality assays showing fertility counts of individual worms at 25°C. **(A)** All four *met-1* alleles generated from the *morc-1* suppressor screen (*xk1-4)* rescue *morc-1(-)* germline mortality. **(B)** *met-1* alleles *xk2* and *xk4* rescue *morc-1(-)* germline mortality. *met-1(xk2)* and *met-1(xk4)* single mutants are fertile at 25°C. **(C)** *met-1* alleles *xk2* and *xk4* rescue *hrde-1(-)* germline mortality. **(D)** Deletion alleles of *met-1* cause severely reduced fertility at 25°C and do not rescue *morc-1(-)* germline mortality. **(E)** RNAi against *met-1* rescues the *morc-1(-)* fertility defect at F7. All error bars indicate mean ± SD, n≥10.

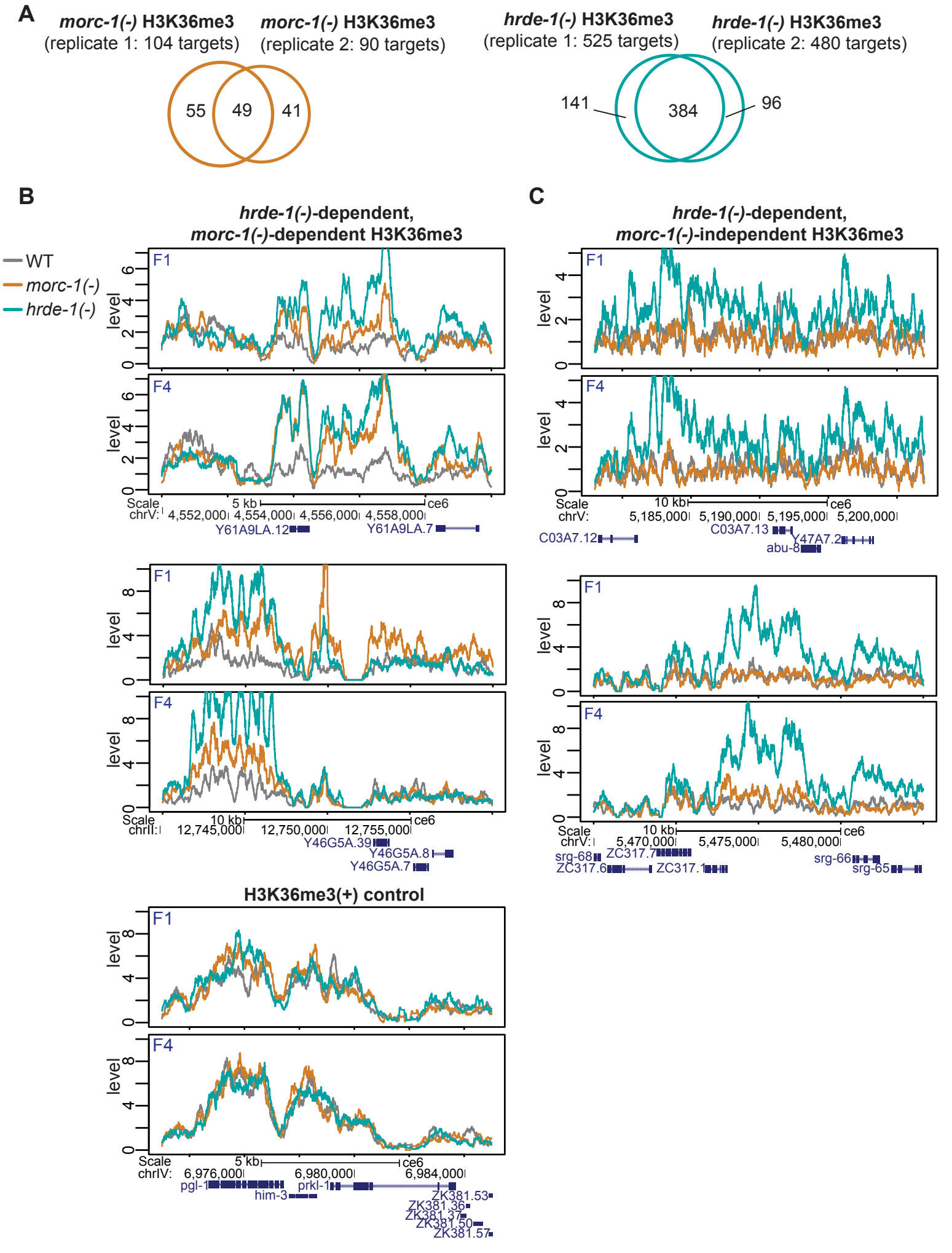
A
morc-1(-) H3K36me3
(replicate 1: 104 targets)
morc-1(-) H3K36me3
(replicate 2: 90 targets)
55
49
41
hrde-1(-) H3K36me3
(replicate 1: 525 targets)
hrde-1(-) H3K36me3
(replicate 2: 480 targets)
141
384
96
B
hrde-1(-)-dependent,
morc-1(-)-dependent H3K36me3
WT
morc-1(-)
hrde-1(-)
F1
F4
level
Scale
chrV:
4,552,000
4,554,000
4,556,000
4,558,000
5 kb
ce6
Y61A9LA.12
Y61A9LA.7
chrII:
12,745,000
12,750,000
12,755,000
10 kb
Y46G5A.39
Y46G5A.8
Y46G5A.7
H3K36me3(+) control
chrIV:
6,976,000
6,980,000
6,984,000
pgl-1
him-3
prkl-1
ZK381.53
ZK381.36
ZK381.37
ZK381.50
ZK381.57
C
hrde-1(-)-dependent,
morc-1(-)-independent H3K36me3
5,185,000
5,190,000
5,195,000
5,200,000
C03A7.12
C03A7.13
Y47A7.2
abu-8
5,470,000
5,475,000
5,480,000
srg-68
ZC317.7
ZC317.6
ZC317.1
srg-66
srg-65

Figure S5. Related to Figures 5 and 6. Regulation of H3K36me3 in *morc-1(-)* and *hrde-1(-)* mutants. (A) Overlap between biological replicates of H3K36me3-enriched regions (fold-change>1.5, FDR<0.05) in F4 mutant compared to wildtype (top: *morc-1(-)* vs. wildtype, bottom: *hrde-1(-)* vs. wildtype). Subsequent analyses were performing using sites that were identified in both biological replicates. **(B)** H3K36me3 levels at exemplary *morc-1(-)*-dependent H3K36me3 regions in early and late generations. At an H3K36me3 positive control region, H3K36me3 levels are unaffected by loss of *morc-1* or *hrde-1*. **(C)** H3K36me3 levels at exemplary *hrde-1(-)*-dependent, *morc-1(-)*-independent H3K36me3 loci in early and late generations (bottom).

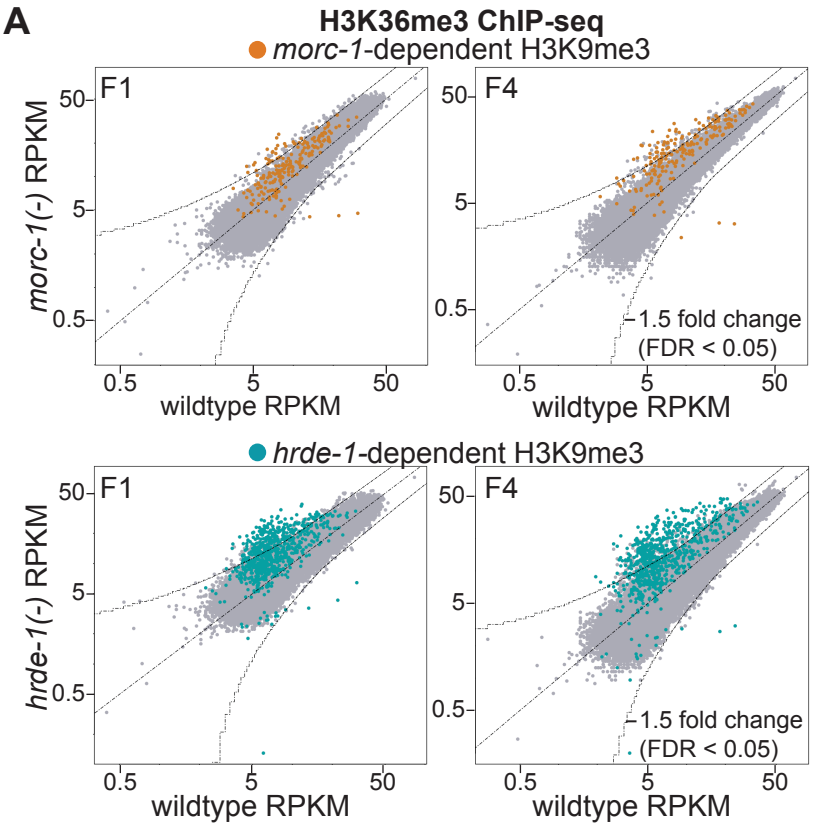
A
H3K36me3 ChIP-seq
morc-1-dependent H3K9me3
F1
F4
morc-1(-) RPKM
wildtype RPKM
1.5 fold change
(FDR < 0.05)
hrde-1-dependent H3K9me3
hrde-1(-) RPKM

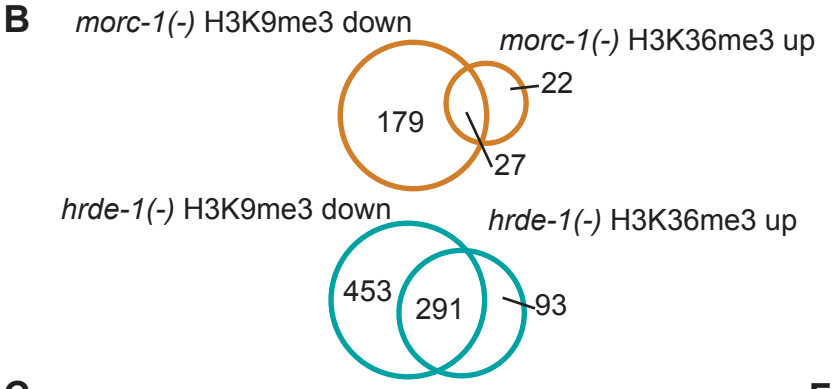
B
morc-1(-) H3K9me3 down
morc-1(-) H3K36me3 up
179
22
27
hrde-1(-) H3K9me3 down
hrde-1(-) H3K36me3 up
453
291
93

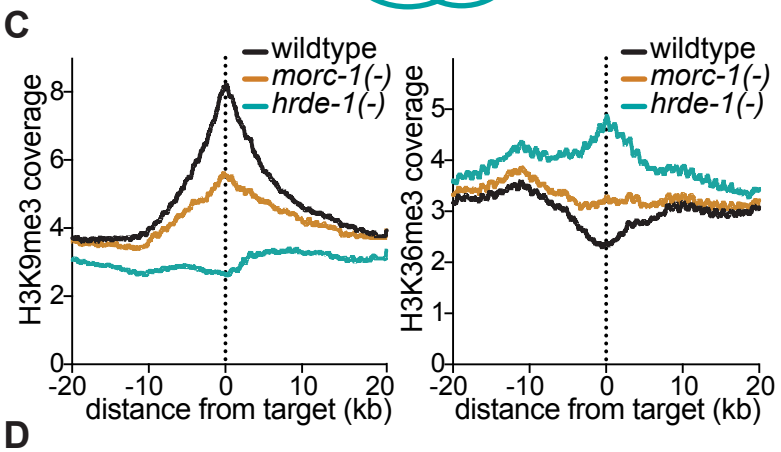
C
wildtype
morc-1(-)
hrde-1(-)
H3K9me3 coverage
H3K36me3 coverage
distance from target (kb)

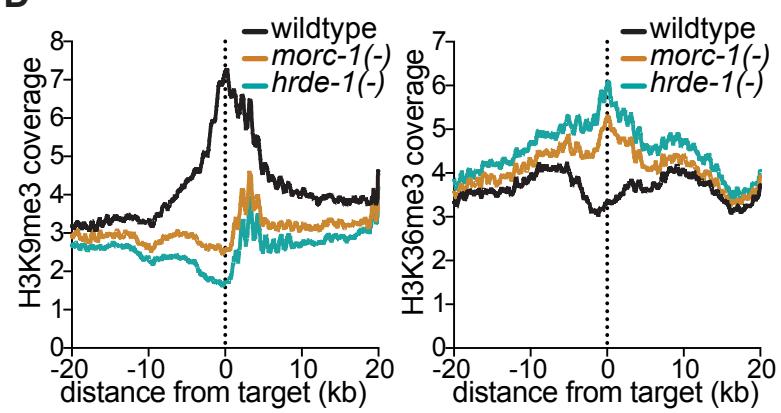
D
wildtype
morc-1(-)
hrde-1(-)
H3K9me3 coverage
H3K36me3 coverage
distance from target (kb)

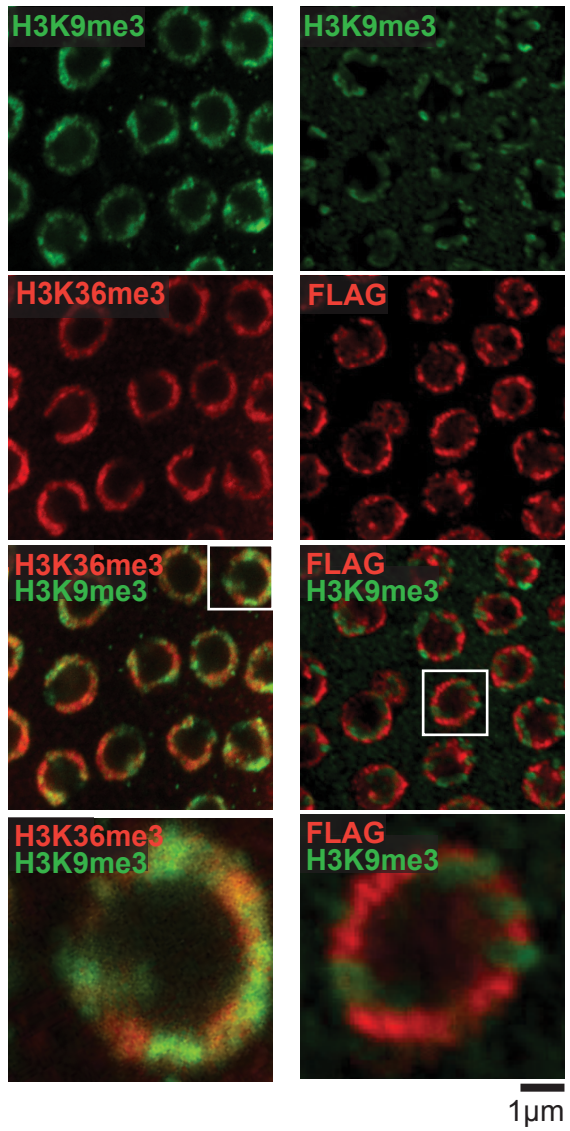
E
10μm
H3K9me3
H3K36me3
FLAG
1μm

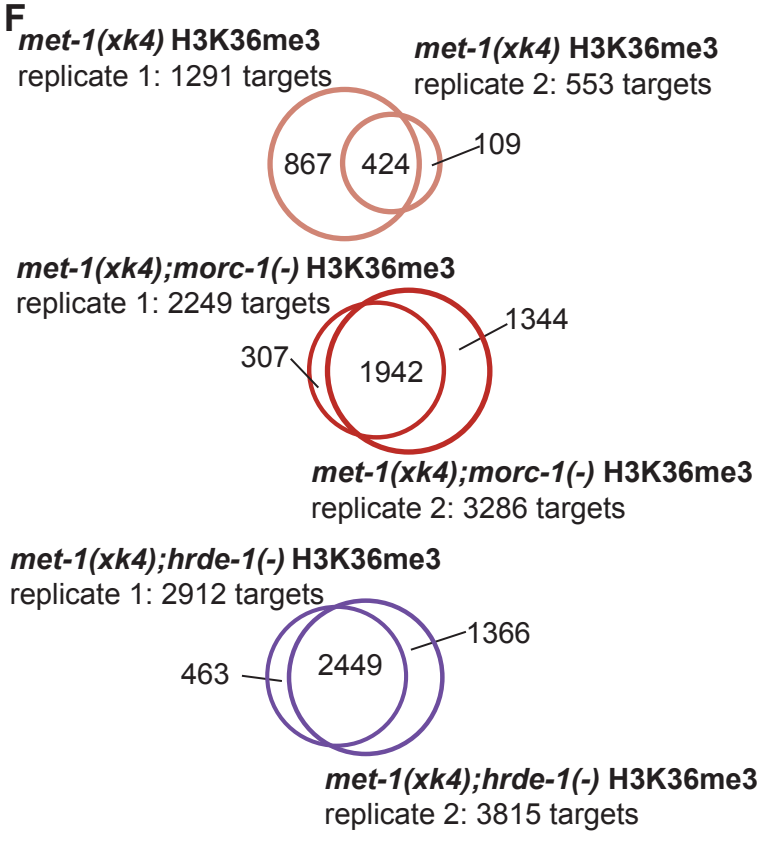
F
met-1(xk4) H3K36me3
replicate 1: 1291 targets
met-1(xk4) H3K36me3
replicate 2: 553 targets
867
424
109
met-1(xk4);morc-1(-) H3K36me3
replicate 1: 2249 targets
307
1942
1344
met-1(xk4);morc-1(-) H3K36me3
replicate 2: 3286 targets
met-1(xk4);hrde-1(-) H3K36me3
replicate 1: 2912 targets
463
2449
1366
met-1(xk4);hrde-1(-) H3K36me3
replicate 2: 3815 targets

Figure S6. Related to Figures 5 and 6. Correlation of changes in H3K9me3 and H3K36me3 levels in *morc-1(-)* and *hrde-1(-)* compared to wildtype. (A) Scatter plots showing H3K36me3 levels in F1 and F4 *morc-1(-)* (top) and *hrde-1(-)* (bottom) vs. wildtype. Regions that are depleted of H3K9me3 in F4 *morc-1(-)* vs. wildtype in two biological replicates are highlighted in yellow. Regions that are depleted of H3K9me3 in F4 *hrde-1(-)* vs. wildtype in two biological replicates are highlighted in blue. **(B)** Overlap between loci that are depleted of H3K9me3 and targets that are enriched for H3K36me3 in late generation *morc-1(-)* (top) and *hrde-1(-)* (bottom) vs. wildtype. **(C)** H3K9me3 (left) and H3K36me3 (right) levels 20 kb upstream and downstream of *hrde-1*-dependent H3K9me3 loci in wildtype, *morc-1(-)*, and *hrde-1(-)* worms at F4 generation. **(D)** H3K9me3 (left) and H3K36me3 (right) levels 20 kb upstream and downstream of *morc-1*-dependent H3K9me3 loci in wildtype, *morc-1(-)*, and *hrde-1(-)* worms at F4 generation. **(E)** Co-immunostaining of H3K36me3 and H3K9me3 (left) resembles the pattern of MORC-1::3xFlag and H3K9me3, which is shown for reference, from a different experiment, at right. **(F)** Overlap of F4 regions that are >1.5-fold depleted of H3K36me3 with FDR<0.05 in two biological replicates of: *met-1(xk4)* vs. wildtype (top), *met-1(xk4);morc-1(-)* vs. *morc-1(-)* (middle), and *met-1(xk4);hrde-1(-)* vs. *hrde-1(-)* (bottom).

Figure S7

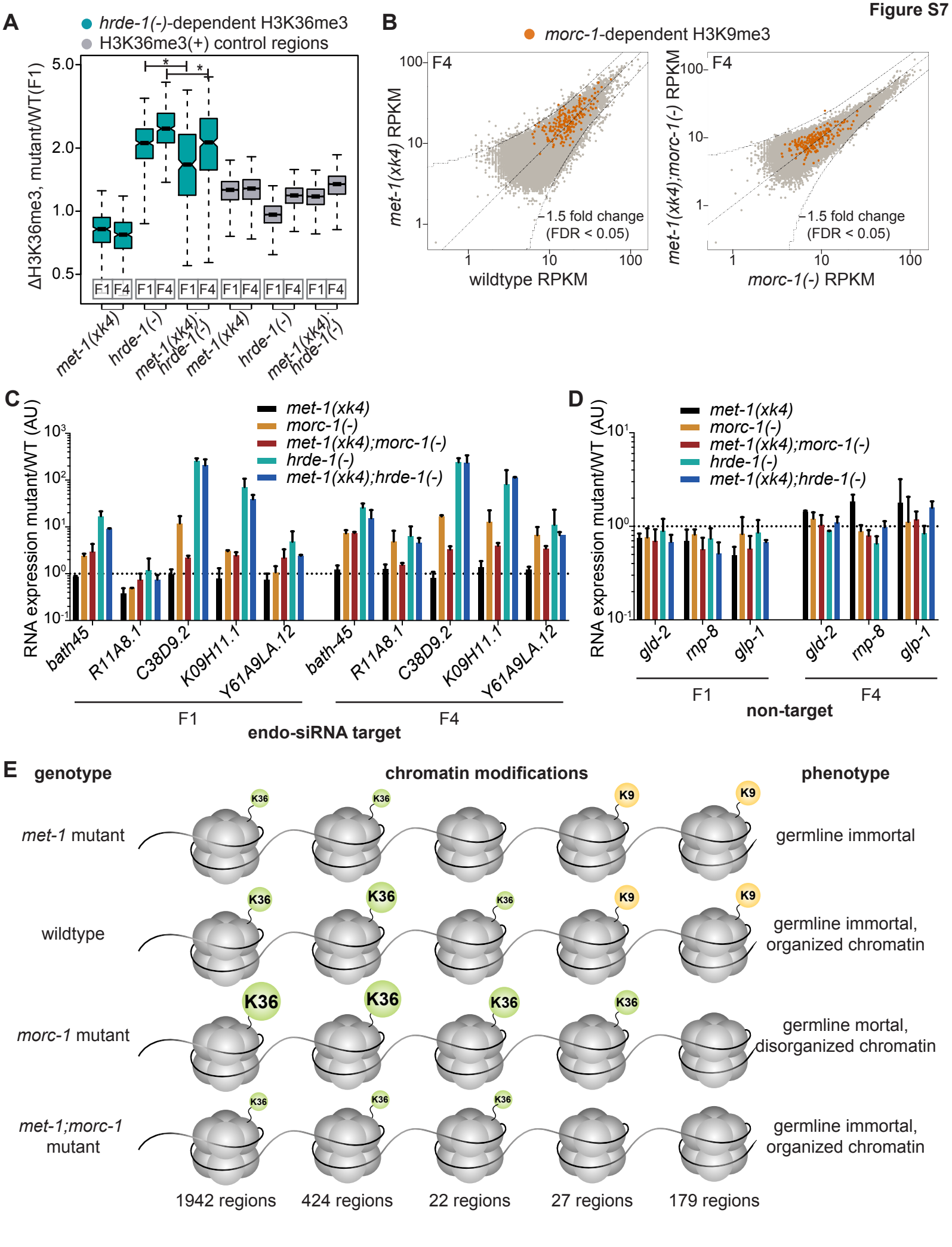
A
hrde-1(-)-dependent H3K36me3
H3K36me3(+) control regions
ΔH3K36me3, mutant/WT(F1)
5.0
2.0
1.0
0.5
F1 F4 F1 F4 F1 F4 F1 F4 F1 F4 F1 F4
met-1(xk4)
hrde-1(-)
met-1(xk4); hrde-1(-)
met-1(xk4)
hrde-1(-)
met-1(xk4); hrde-1(-)
B
morc-1-dependent H3K9me3
F4
met-1(xk4) RPKM
wildtype RPKM
1.5 fold change (FDR < 0.05)
met-1(xk4);morc-1(-) RPKM
morc-1(-) RPKM
C
met-1(xk4)
morc-1(-)
met-1(xk4);morc-1(-)
hrde-1(-)
met-1(xk4);hrde-1(-)
RNA expression mutant/WT (AU)
bath45
R11A8.1
C38D9.2
K09H11.1
Y61A9LA.12
F1
F4
endo-siRNA target
D
gld-2
rnp-8
glp-1
non-target
E
genotype
chromatin modifications
phenotype
met-1 mutant
germline immortal
wildtype
germline immortal, organized chromatin
morc-1 mutant
germline mortal, disorganized chromatin
met-1;morc-1 mutant
germline immortal, organized chromatin
K36
K9
1942 regions
424 regions
22 regions
27 regions
179 regions

Figure S7. Related to Figure 6. MET-1 drives H3K36me3 gain but not H3K9me3 loss or mRNA upregulation in nuclear RNAi mutants (A) Box plot showing H3K36me3 levels at *hrde-1(-)*-dependent H3K36me3 loci in the indicated mutant background and generation relative to wildtype F1. These regions are significantly depleted in *met-1(xk4);hrde-1(-)* compared to *hrde-1(-)* at both generations (F1 p=3.28x10^{-14}, F4 p=1.15x10^{-10}, Welch's t-test). Gray boxes show H3K36me3 levels in regions with highest H3K36me3 in F1 wildtype. **(B)** Scatter plots comparing H3K9me3 levels in *met-1(xk4)* vs. wildtype (left) and *met-1(xk4);morc-1(-)* vs. *morc-1(-)* in F4 generation show that *met-1* does not affect H3K9me3 levels. Sites that were identified as *morc-1*-dependent for H3K9me3 (Figure 3A) are highlighted in yellow. **(C)** qRT-PCR of endo-siRNA target genes in the indicated mutant backgrounds in F1 and F4 generations. Expression levels were normalized to *eft-2* levels and are shown relative to wildtype of the indicated generation (mean ± SD of two technical replicates). Levels of germline-expressed mRNAs that are not endo-siRNA targets are shown in **(D)**. **(E)** Model of MORC-1 and MET-1 effects on chromatin modifications and fertility.